

promoting access to White Rose research papers



Universities of Leeds, Sheffield and York
<http://eprints.whiterose.ac.uk/>

This is the author's version of an article published in **International Journal of Hydrogen Energy**

White Rose Research Online URL for this paper:

<http://eprints.whiterose.ac.uk/id/eprint/75918>

Published article:

Wu, C, Williams, PT and Huang, J (2013) *Carbon nanotubes and hydrogen production from the reforming of toluene*. International Journal of Hydrogen Energy. ISSN 0360-3199

<http://dx.doi.org/10.1016/j.ijhydene.2013.05.028>

Carbon nanotubes and hydrogen production from the reforming of toluene

Chunfei Wu^{a,*}, Jun Huang^{b,*}, Paul T. Williams^{a,*}

^aEnergy Research Institute, The University of Leeds, Leeds, LS2 9JT, UK

(Tel: #44 1133432504; Email: p.t.williams@leeds.ac.uk; c.wu@leeds.ac.uk)

^bLaboratory for Catalysis Engineering, School of Chemical and Biomolecular Engineering,

The University of Sydney, NSW 2006, Australia

(Tel: #61 2 9351 7483; Email: jun.huang@sydney.edu.au)

Abstract:

Catalytic steam reforming of liquid hydrocarbons is one of the promising alternatives for hydrogen production. However, coke deposition on the reacted catalyst results in catalyst deactivation and also CO₂ emission during reforming are among the main challenges in the process. In this work, the production of high-value carbon nanotubes (CNTs) during hydrogen production from catalytic reforming of toluene has been investigated. Thus, less carbon emission and higher product values can be expected from the process. A two-stage fixed bed pyrolysis-reforming reactor was used in this work. The results showed that the addition of a Ni-Mg-Al catalyst, with an additional downstream stainless steel mesh, increased hydrogen production from 24.8 to 54.8 (mmol H₂ g⁻¹ toluene), when water (steam) was injected at a rate of 0.01 g min⁻¹. CNTs were also produced in the process in the presence of the Ni-Mg-Al catalyst and with a water injection rate of 0.01 g min⁻¹ had the highest band ratio of G'/G when analysed by Raman spectrometry, indicating the highest purity of CNTs. In addition, Raman spectra of the generated CNTs showed that the purity of CNTs was reduced with the addition of water for reforming without the Ni-Mg-Al catalyst. The presence of the Ni-Mg-Al catalyst significantly increased the yield of CNTs formed on the surface of the stainless steel mesh and also improved the quality of the CNTs in relation to the distribution of diameters and their length.

Key Words: Hydrogen; Gasification; Toluene; Carbon Nanotubes

1. Introduction

Alternative clean energy is in high demand due to the economic and political concerns of long-term fossil fuel shortages and environmental impact caused by using fossil fuels [1]. Hydrogen is regarded as one of the most promising energy carriers for clean fuels, since its combustion only generates water and importantly, it can be produced from various renewable materials such as biomass [2, 3]. Hydrogen production, storage, distribution and its use in energy applications have been extensively researched [2, 4, 5].

Gasification/reforming of liquid hydrocarbon materials such as biomass tar and waste derived hydrocarbon oils from wastes such as plastics and tyres have been investigated for hydrogen production [6-12]. Catalyst is known to be important for improving hydrogen production from gasification/reforming process; especially nickel-based catalyst is widely used for its effective catalytic activities of hydrocarbons conversion and hydrogen production. However, coke deposition (amorphous carbons, heavy hydrocarbons and filamentous carbons etc.) on the surface of the catalyst has caused deactivation of the catalyst [6, 12]. A large amount of research has been carried out to investigate and reduce coke formation [13-15]. In addition, CO₂ emission is not avoidable in the process of hydrogen production from gasification/reforming; the emission of CO₂ impacts climate change and reduces the overall efficiency of the gasification/reforming process.

This paper introduces a novel process that has the potential to convert hydrocarbon liquids into hydrogen and also high-value carbon nanotubes (CNTs). Co-production of hydrogen and CNTs has been reported with the reforming of ethanol [16, 17]. However, few studies could be found for the reforming of other liquid hydrocarbons. We recently reported that CNTs could be generated as a by-product of hydrogen from pyrolysis-gasification of waste plastics [18]. CNTs have unique physical and chemical properties and have received increasing recent interest, and are predicted to have many applications in the areas of hydrogen storage [19], reinforced composites and carbon electrodes [20] and biosensors [21] etc. Therefore, high-value CNTs add significant economic value to the hydrogen production from reforming of hydrocarbons.

This research seeks to demonstrate whether, and how, high-quality CNTs and hydrogen are produced from steam reforming of toluene as a representative model compound of hydrocarbon oil. For example, toluene has been used as a model compound of tar oil for gasification research [22-27] Toluene has also known as a common compound in tyre pyrolysis oil at about 3.6 wt.% [28] and for catalytically upgraded tyre pyrolysis oils can reach concentrations of ~24% [29-31]. Toluene is also found in the liquid oils derived from the pyrolysis of waste plastics at concentrations of 7.6 wt.% [32].

A two-stage reactor system was used for the experimentation, where the toluene was pre-heated in the first stage followed by steam reforming of the pre-heated gases in the second stage in the presence of a Ni-Mg-Al catalyst; the catalyst was selected due to its effective catalytic effect for hydrogen production from plastics gasification from our previous work [15, 33, 34]. Stainless steel has been reported for the growth of CNTs [35, 36]; in this work, it was investigated for the purpose of promoting CNTs production. In addition, steam addition was also studied to determine its influence on hydrogen and CNTs production from catalytic toluene reforming.

2. Materials and methods

2.1. Materials

Toluene was purchased from Merck and used as the model compound of hydrocarbon liquids. Stainless steel gauze (400 mesh woven from 0.028 mm diameter wire), purchased from Alfa Aesar, was used as a catalyst for the generation of CNTs. The stainless steel mesh was cut to small squares ~4 mm, immersed in 10 % nitric acid and washed with de-ionized water. Before use in the gasification experiments, the stainless steel mesh was dried at 100 °C overnight and also pre-treated at 800 °C for 3 h in an air atmosphere.

Ni-Mg-Al catalyst was prepared by a co-precipitation method. $\text{Ni}(\text{NO}_3)_2 \cdot 6\text{H}_2\text{O}$, $\text{Al}(\text{NO}_3)_3 \cdot 9\text{H}_2\text{O}$ and $\text{Mg}(\text{NO}_3)_2 \cdot 6\text{H}_2\text{O}$ were dissolved into de-ionized water and $\text{NH}_4(\text{OH})$ solution was added to the nitrate solution until the pH reached 8.3. The precipitates were filtered with water, followed by drying at 105 °C overnight, and then were calcined in an air atmosphere at 750 °C for 3h. The Ni/Mg/Al molar ratio of the catalyst was 1:1:1.

2.2. Methods

Toluene reforming experiments were carried out using a two-stage fixed-bed reaction system (Fig. 1), which is similar to other report [37]. N_2 was used as a carrier gas with a flow rate of 80 ml min^{-1} . The gas hourly space velocity was around 4800 h^{-1} for the experiments. Toluene and water were injected to a mixer using a HPLC pump and syringe pump, respectively. Toluene was pre-heated at around $250 \text{ }^\circ\text{C}$ in the first reactor; the derived gases were reformed at around $800 \text{ }^\circ\text{C}$ in a second reactor. In the second reactor, Ni-Mg-Al catalyst, if used, was placed on the top of the stainless steel mesh (0.5 g), separated by quartz wool. The condensable liquids were condensed and the non-condensable gases were collected in a gas sample bag and analyzed off-line by packed column gas chromatography (Varian 3380).

The CNTs deposited on the reacted catalyst were characterized by a high resolution scanning electron microscope (SEM, LEO 1530) coupled with energy dispersive X-ray spectroscopy (EDXS) and a transmission electron microscope (TEM) (Philips CM200). Temperature-programmed oxidation (TPO) was carried out using a Stanton-Redcroft thermogravimetric analyser (TGA and DTG) to determine the properties of the CNTs deposited on the reacted catalysts. Raman spectra of the CNTs were obtained using a Renishaw Invia equipment at a wavelength of 514 nm .

3. Results and discussion

3.1. Product yield

In this work, various water injection rates ($0.00, 0.01, 0.05$ and 0.1 g min^{-1}) were investigated for the production of CNTs and hydrogen from toluene reforming in the presence/absence of the Ni-Mg-Al catalyst. Experimental conditions, mass balances and gas concentrations are shown in Table 1.

3.1.1. Gas and hydrogen production.

Gas yield was increased from around 16.1 to $58.4 \text{ wt.}\%$ and hydrogen production was increased from 22.9 to $24.8 \text{ (mmol H}_2 \text{ g}^{-1} \text{ toluene)}$ when water was injected into the reaction system with a flow rate of 0.01 g min^{-1} , in the absence of the Ni-Mg-Al catalyst, but with the

stainless steel mesh in place. The gas yield was calculated by the mass of non-condensed gases divided by the injected toluene. The hydrogen production was calculated as the molar of hydrogen produced by the mass of total injected toluene. However, when the water injection rate was increased up to 0.1 g min^{-1} (still without the Ni-Mg-Al catalyst), gas and hydrogen production was obviously reduced (Table 1). Even in the presence of the Ni-Mg-Al catalyst, when the water injection rate was increased from 0.01 to 0.05 g min^{-1} gas production was also reduced from 105.5 to $69.0 \text{ wt.}\%$ with reduced hydrogen production from 58.4 to 31.0 ($\text{mmol H}_2 \text{ g}^{-1}$ toluene). The results indicate that hydrogen production from the toluene steam reaction was prohibited in the presence of high amounts of steam. The saturation of the catalyst surface by steam has been suggested at high steam/carbon ratios when investigated in the process of steam reforming of toluene [38] and benzene [39].

As shown in Table 1, when the Ni-Mg-Al catalyst was introduced into the reforming process, gas production was dramatically increased from 58.4 to $105.5 \text{ wt.}\%$ with enhanced hydrogen production from 24.8 to 54.8 ($\text{mmol H}_2 \text{ g}^{-1}$ toluene) with the injection of 0.01 g min^{-1} water. Therefore, we suggest that the Ni-Mg-Al catalyst used in this work significantly improves the production of hydrogen during toluene reforming. This observation fits well with previous reports that commercial Ni-based catalysts promote high yields of hydrogen during the steam reforming of oil derived from biomass pyrolysis [40].

3.1.2. Carbon production

In this work, valuable CNT materials were detected in addition to hydrogen production during reforming of toluene as a model compound of hydrocarbon liquids. The materials were collected in the reactor after the reforming process, and the amount has been summarized in Table 1.

From Table 1, the influence of water injection rate on toluene reforming has been found to significantly influence the production of CNTs on the stainless steel mesh. In the absence of the Ni-Mg-Al catalyst, the carbon materials on the stainless steel mesh have been obtained without water injection with carbon conversion to CNTs (about $43.8 \text{ wt.}\%$); their production was reduced when water was injected at 0.01 g min^{-1} (with S/C ratio of 0.7) (CNTs production $<5 \text{ wt.}\%$); furthermore, CNTs disappeared when water was introduced at higher flow rate (0.1 g min^{-1}) (with S/C ratio of 7.3) into the non-catalytic experiment.

However, when the Ni-Mg-Al catalyst was placed in the reforming process with a water injection rate of 0.01 g min^{-1} , a higher production of CNTs was obtained on the surface of the stainless steel mesh (~56.9 wt.% of the carbons in the feedstock toluene were converted into CNTs). Therefore, the presence of the Ni-Mg-Al catalyst is essential for the production of CNTs in this work. It has to be pointed out that coke formation was also observed on the reacted Ni-Mg-Al catalyst from SEM analysis (not shown here). In this work, CNTs formation is focused on the stainless steel, detailed analysis of the catalyst stability is needed for the stability of the Ni-Mg-Al catalyst.

A vapor-liquid-solid mechanism has been initially developed by Baker et al. [41, 42] for the growth of carbon nanofibres: a carbon containing gas precursor generates carbon atoms on the surface of the catalyst; a liquid carbide is formed through the carbon atoms dissolution; finally, solid carbon precipitates with the nanoparticles to form carbon filaments. However, the driving force for the diffuse of carbon atoms through nanoparticles is not clear [43]. Tibbetts [44] proposed that a difference of carbon solubility at the gas/metal interface and the carbon/metal interface - a carbon concentration gradient, is the driving force for the carbon diffusion.

However, with the further increase of the water injection rate to 0.05 g min^{-1} , the carbon material could barely be found, even in the presence of the Ni-Mg-Al catalyst. We suggested that the toluene conversion was improved in the presence of the catalyst; since catalyst has been reported to increase toluene conversion [38]. The precursors derived from catalytic reforming of toluene are suggested to be favorable for the CNTs production on the surface of the stainless steel mesh. In addition, the CO_2 concentration was reduced when the Ni-Mg-Al catalyst was added to the experiment with water injection rate of 0.01 g min^{-1} compared with the non-catalytic experiment (Table 1). This is further to prove that more carbons were converted into CNTs.

3.2. SEM analysis

3.2.1. Influence of water injection

The reacted stainless steel meshes were analyzed with SEM, and the images are shown in Fig. 2 and 3. For the reacted stainless steel mesh with water injection rate higher than 0.05 g min^{-1} , CNTs were difficult to identify (Fig. 3); however, CNTs could be clearly observed on the reacted stainless steel mesh when the water injection rate was 0.01 g min^{-1} or without water injection in the absence of the Ni-Mg-Al catalyst (Fig. 2). When the water injection rate was increased from 0.01 to 0.05 g min^{-1} (S/C ratio increased from 0.0 to 3.7) in the presence of the Ni-Mg-Al catalyst, CNTs were barely detected (Fig. 2 and 3).

It has been reported that suitable amounts of water addition into the CNTs production process could increase the length of the CNTs; it has been proposed that the oxidant (H_2O) has an etching effect on the carbon species that are not consumed by the formation of the CNTs which may deactivate the metal particles [45]. However, at higher concentrations of H_2O , the oxidant has also been reported to etch the CNTs [46]; therefore, CNTs are suggested to be etched by water at a high water injection rate (0.05 g min^{-1}) in this work.

3.2.2. Influence of the addition of the Ni-Mg-Al catalyst

As shown in Fig. 2, coiled CNTs were found on the reacted stainless steel mesh without catalyst and without water injection. When water was injected with 0.01 g min^{-1} to the toluene reforming system without catalyst, the diameter of the CNTs was larger and the length of the CNTs becomes shorter. In the presence of the Ni-Mg-Al catalyst with the water injection rate of 0.01 g min^{-1} , CNTs with narrow diameter distribution were found on the stainless steel mesh; additionally, the length of the produced CNTs could be more than $20 \text{ }\mu\text{m}$.

Therefore, it seems that the introduction of water and/or the Ni-Mg-Al catalyst into the toluene reforming process significantly influences the growth of the CNTs. When a carbon nucleus was formed, the available carbon was concluded to have three possible routes [47]: (1) continuously grow with the original carbon cap; (2) form a new carbon cap until energetically unfavorable; (3) add to the cylindrical part of the tube.

In this contribution, when water was injected at 0.01 g min^{-1} without the Ni-Mg-Al catalyst, for the steam reforming of toluene, dissolved carbon seems to be added to the cylindrical section of the originally formed CNTs, thus the diameter of the CNTs was increased with relative short lengths (Fig. 2 (b)). Conversely, dissolved carbons were added to the cap of the

initially formed CNTs on the surface of the stainless steel mesh, and produced longer but narrower CNTs, when the Ni-Mg-Al catalyst was added into the reaction system at the water injection rate of 0.01 g min^{-1} (Fig. 2 (c) (d)).

Interestingly, a narrow distribution of CNTs could also be observed from TEM images (Fig. 4), where CNTs were found with diameters of around 20 nm. About 14 graphene layers parallel to the axis of the CNT were found, clearly indicating that tubular multi-walled CNTs were produced from the catalytic reforming of toluene in the presence of the stainless steel mesh. Similar production of aligned CNTs on the stainless steel mesh has been obtained, when ethane and hydrogen were used as feedstock [48]. Compared to non-catalytic toluene reforming, the introduction of the Ni-Mg-Al catalyst increased the production and improved the quality of the CNTs in terms of a narrower diameter distribution and increased length, while the hydrogen production was also significantly increased.

3.3. Raman analysis

Raman spectra of CNTs are shown in Fig. 5. The D band at 1350 cm^{-1} is assigned to disordered carbon structures, and the G band at around 1575 cm^{-1} is attributed to graphite carbons.[49] The second order Raman spectrum G' band at around 2683 cm^{-1} is due to the two-photon elastic scattering process [50]. The intensity of G' band is particularly related to the purity of the CNTs, as two-photon elastic scattering would not happen with a disordered sample [49]. Raman mode at around 2930 cm^{-1} is suggested to be a combination mode of the D and G modes [51].

In the absence of the Ni-Mg-Al catalyst, the high intensity of the D band for the reacted stainless steel mesh (Fig. 5 (b)) indicates that the amount of disordered carbons were increased with the water injection rate of 0.01 g min^{-1} , compared with the non-steam toluene reforming (Fig. 5 (a)). Additionally, the low intensity of the G' band (IG'/IG , 0.46) (Fig. 5 (b)) also demonstrates that poor purity of the CNTs was obtained, when water (0.01 g min^{-1}) was added to toluene reforming in the absence of the Ni-Mg-Al catalyst.

The lowest ratio of intensity of the D to G band (ID/IG , 0.56) and the highest ratio of IG'/IG (0.73) were obtained and shown in Fig. 5 (c); thus indicating that the CNTs, derived from toluene reforming process in the presence of the Ni-Mg-Al catalyst and with a water injection

rate of 0.01 g min^{-1} , have the highest purity and lowest disordered carbons among the produced CNTs in this work. It is also further demonstrated that the Ni-Mg-Al catalyst has a positive effect on the formation of CNTs. The Ni-Mg-Al catalyst reformed the toluene and might generate hydrocarbons which are favorable to form CNTs on the surface of the stainless steel mesh. It is proposed that the increased hydrogen content with the addition of the Ni-Mg-Al catalyst in the gas stream might prevent the sintering of Fe particles on the stainless steel mesh; thus resulting in the growth of long and uniform CNTs, compared with the experiment without the Ni-Mg-Al catalyst.

3.4. Temperature programmed oxidation of CNTs.

A single oxidation peak was observed for the produced CNTs from toluene reforming with and without the Ni-Mg-Al catalyst (Fig. 6). From Fig. 6, the TPO peak moved to higher temperature for the CNTs generated in the presence of the Ni-Mg-Al catalyst. Herrera et al. [52] reported that the presence of metal species in the CNTs catalyze the oxidation reaction during their TPO experiment. In this work, the presence of Fe metals has been observed from the EDXS analysis of the CNTs (Fig. 7). Iron oxides are also observed after TPO analysis. Additionally, less Fe metal species were found in the CNTs generated with the Ni-Mg-Al catalyst (Fig.7 (b)). Therefore, the move of the TPO oxidation peak to higher temperature for the CNTs obtained in the presence of the Ni-Mg-Al catalyst might be due to the lower content of Fe species in the CNTs. Furthermore, the sharp oxidation peak of the TPO analysis was observed for the CNTs produced with the Ni-Mg-Al catalyst (Fig. 6 (c)). It is further indicated that the CNTs, produced in the presence of the Ni-Mg-Al catalyst at a water injection rate of 0.01 g min^{-1} , have a comparatively narrow diameter distribution (as shown in SEM analysis, Fig. 2 and 3).

3.5. Toluene reforming with high material feeding rate

From the above analysis and discussions, the presence of catalyst and water injection rate have significantly influence on the CNTs production. Here, we studied the steam reforming of toluene at higher ratio of toluene/catalyst with a modified water/toluene ratio (toluene injection rate: 0.07 g min^{-1} ; water injection rate 0.02 g min^{-1}). Hydrogen production and concentration were 35.6 and 18.5 Vol.%, respectively (Table 1). The hydrogen production was reduced with the increase of feeding rate of toluene, as less catalytic sites were available

at higher feeding rate of raw material. As shown in Table 1, higher carbon conversion to CNTs (~70.4 wt.%) was obtained at higher feeding rate of toluene, which was ascribed to the lower ratio of catalyst/toluene and also steam/toluene.

Interestingly, CNTs with uniform distribution of diameters are observed from the SEM analysis, as shown in Fig. 8; additionally, the length of the CNTs could be more than 50 μm . Compared with a lower feeding rate of toluene (Fig. 2), the CNTs obtained from the higher toluene feeding rate (0.07 g min^{-1}) are with longer length; indicating the CNTs have been grown on the surface of stainless steel mesh while the diameter of CNTs kept constant. In addition, the produced CNTs could be easily physically separated from the stainless steel mesh, as gram quantities of CNTs powder were collected after the experiment. Therefore, producing high quality CNTs from steam reforming of toluene was proved to be possible in this work by manipulating the processing conditions such as catalyst, steam and material feeding rate.

4. Conclusions

In summary, high-quality CNTs with a narrow diameter distribution and up to 50 μm in length were generated from the steam reforming of toluene as a representative hydrocarbon liquid model compound in the presence of a Ni-Mg-Al catalyst and stainless steel mesh. The introduction of the Ni-Mg-Al catalyst has a positive effect for CNTs production by modifying the carbon sources before deposition onto the stainless steel mesh. In addition, higher hydrogen production was also obtained when the Ni-Mg-Al catalyst was added to the reforming process.

Hydrogen production was increased with the increase of water injection; however, the amount of CNTs was reduced. Increasing the feeding rate of toluene resulted in the increase of the length and the production yield of CNTs.

Acknowledgements

This work was supported by the International Exchange Scheme from the Royal Society (IE110273), and the Early Career Research Scheme from the University of Sydney.

References

- [1] Urbaniec K, Friedl A, Huisingh D, Claassen P. Hydrogen for a sustainable global economy. *Journal of Cleaner Production*. 2010;18, Supplement 1:S1-S3.
- [2] Sherif SA, Barbir F, Veziroglu TN. Wind energy and the hydrogen economy—review of the technology. *Solar Energy*. 2005;78:647-60.
- [3] Seth D. Hydrogen futures: toward a sustainable energy system. *International Journal of Hydrogen Energy*. 2002;27:235-64.
- [4] Leaver J, Gillingham K. Economic impact of the integration of alternative vehicle technologies into the New Zealand vehicle fleet. *Journal of Cleaner Production*. 2010;18:908-16.
- [5] Sun Z-y, Liu F-S, Liu X-h, Sun B-g, Sun D-W. Research and development of hydrogen fuelled engines in China. *International Journal of Hydrogen Energy*. 2012;37:664-81.
- [6] Elbaba IF, Wu C, Williams PT. Hydrogen production from the pyrolysis-gasification of waste tyres with a nickel/cerium catalyst. *International Journal of Hydrogen Energy*. 2011;36:6628-37.
- [7] Conesa JA, Martin-Gullon I, Font R, Jauhiainen J. Complete study of the pyrolysis and gasification of scrap tires in a pilot plant reactor. *Environmental Science & Technology*. 2004;38:3189-94.
- [8] Elbaba IF, Williams PT. Two stage pyrolysis-catalytic gasification of waste tyres: Influence of process parameters. *Applied Catalysis B-Environmental*. 2012;125:136-43.
- [9] Elbaba IF, Wu C, Williams PT. Catalytic Pyrolysis-Gasification of Waste Tire and Tire Elastomers for Hydrogen Production. *Energy & Fuels*. 2010;24:3928-35.
- [10] Yoon SJ, Choi Y-C, Lee J-G. Hydrogen production from biomass tar by catalytic steam reforming. *Energy Conversion and Management*. 2010;51:42-7.
- [11] Zhao B, Zhang X, Chen L, Qu R, Meng G, Yi X, et al. Steam reforming of toluene as model compound of biomass pyrolysis tar for hydrogen. *Biomass & Bioenergy*. 2010;34:140-4.
- [12] Wu C, Williams PT. Pyrolysis-gasification of post-consumer municipal solid plastic waste for hydrogen production. *International Journal of Hydrogen Energy*. 2010;35:949-57.
- [13] Müller JB, Vogel F. Tar and coke formation during hydrothermal processing of glycerol and glucose. Influence of temperature, residence time and feed concentration. *The Journal of Supercritical Fluids*. 2012;70:126-36.

- [14] Zhang Y, Kajitani S, Ashizawa M, Oki Y. Tar destruction and coke formation during rapid pyrolysis and gasification of biomass in a drop-tube furnace. *Fuel*. 2010;89:302-9.
- [15] Wu C, Williams PT. Investigation of coke formation on Ni-Mg-Al catalyst for hydrogen production from the catalytic steam pyrolysis-gasification of polypropylene. *Applied Catalysis B: Environmental*. 2010;96:198-207.
- [16] Wang G, Wang H, Li W, Bai J. Preparation of hydrogen and carbon nanotubes over cobalt-containing catalysts via catalytic decomposition of ethanol. *RSC Advances*. 2011;1:1585-92.
- [17] Wang G, Wang H, Li W, Ren Z, Bai J, Bai J. Efficient production of hydrogen and multi-walled carbon nanotubes from ethanol over Fe/Al₂O₃ catalysts. *Fuel Processing Technology*. 2011;92:531-40.
- [18] Wu C, Wang Z, Wang L, Williams PT, Huang J. Sustainable processing of waste plastics to produce high yield hydrogen-rich synthesis gas and high quality carbon nanotubes. *RSC Advances*. 2012;2:4045-7.
- [19] Brown M. Carbon nanotubes for hydrogen storage. *Chemistry World*. 2011;8:20-20.
- [20] Noked M, Okashy S, Zimrin T, Aurbach D. Composite Carbon Nanotube/Carbon Electrodes for Electrical Double-Layer Super Capacitors. *Angewandte Chemie-International Edition*. 2012;51:1568-71.
- [21] Baughman RH, Zakhidov AA, de Heer WA. Carbon Nanotubes--the Route Toward Applications. *Science*. 2002;297:787-92.
- [22] Bassil G, Mokbel I, Abou Naccoul R, Stephan J, Jose J, Goutaudier C. Tar removal from biosyngas in the biomass gasification process. (Liquid plus liquid) equilibrium {water plus solvent (paraxylene and methyl hexadecanoate) plus model molecules of tar (benzene, toluene, phenol)}. *Journal of Chemical Thermodynamics*. 2012;48:123-8.
- [23] Kong M, Fei J, Wang S, Lu W, Zheng X. Influence of supports on catalytic behavior of nickel catalysts in carbon dioxide reforming of toluene as a model compound of tar from biomass gasification. *Bioresource Technology*. 2011;102:2004-8.
- [24] Kong M, Yang Q, Fei J, Zheng X. Experimental study of Ni/MgO catalyst in carbon dioxide reforming of toluene, a model compound of tar from biomass gasification. *International Journal of Hydrogen Energy*. 2012;37:13355-64.
- [25] Thassanaprichayanont S, Atong D, Sricharoenchaikul V. Alumina Supported Ni-Mg-La Tri-Metallic Catalysts for Toluene Steam Reforming as a Biomass Gasification Tar Model Compound. In: Gan B, Gan Y, Yu Y, editors. *Applied Materials and Electronics Engineering*, Pts 1-22012. p. 614-8.

- [26] Virginie M, Courson C, Kiennemann A. Toluene steam reforming as tar model molecule produced during biomass gasification with an iron/olivine catalyst. *Comptes Rendus Chimie*. 2010;13:1319-25.
- [27] Virginie M, Courson C, Niznansky D, Chaoui N, Kiennemann A. Characterization and reactivity in toluene reforming of a Fe/olivine catalyst designed for gas cleanup in biomass gasification. *Applied Catalysis B-Environmental*. 2010;101:90-100.
- [28] Kaminsky W, Mennerich C, Zhang Z. Feedstock recycling of synthetic and natural rubber by pyrolysis in a fluidized bed. *Journal of Analytical and Applied Pyrolysis*. 2009;85:334-7.
- [29] Williams PT, Brindle AJ. Aromatic chemicals from the catalytic pyrolysis of scrap tyres. *Journal of Analytical and Applied Pyrolysis*. 2003;67:143-64.
- [30] Williams PT, Brindle AJ. Catalytic pyrolysis of tyres: influence of catalyst temperature. *Fuel*. 2002;81:2425-34.
- [31] López G, Olazar M, Aguado R, Bilbao J. Continuous pyrolysis of waste tyres in a conical spouted bed reactor. *Fuel*. 2010;89:1946-52.
- [32] Kaminsky W, Kim J-S. Pyrolysis of mixed plastics into aromatics. *Journal of Analytical and Applied Pyrolysis*. 1999;51:127-34.
- [33] Wu C, Williams PT. Investigation of Ni-Al, Ni-Mg-Al and Ni-Cu-Al catalyst for hydrogen production from pyrolysis–gasification of polypropylene. *Applied Catalysis B: Environmental*. 2009;90:147-56.
- [34] Wu C, Williams PT. Hydrogen production by steam gasification of polypropylene with various nickel catalysts. *Applied Catalysis B: Environmental*. 2009;87:152-61.
- [35] Sano N, Hori Y, Yamamoto S, Tamon H. A simple oxidation–reduction process for the activation of a stainless steel surface to synthesize multi-walled carbon nanotubes and its application to phenol degradation in water. *Carbon*. 2012;50:115-22.
- [36] Amadou J, Begin D, Nguyen P, Tessonnier JP, Dintzer T, Vanhaecke E, et al. Synthesis of a carbon nanotube monolith with controlled macroscopic shape. *Carbon*. 2006;44:2587-9.
- [37] Botas JA, Serrano DP, García A, Ramos R. Catalytic conversion of rapeseed oil for the production of raw chemicals, fuels and carbon nanotubes over Ni-modified nanocrystalline and hierarchical ZSM-5. *Applied Catalysis B: Environmental*. (In press)
- [38] Świerczyński D, Libs S, Courson C, Kiennemann A. Steam reforming of tar from a biomass gasification process over Ni/olivine catalyst using toluene as a model compound. *Applied Catalysis B: Environmental*. 2007;74:211-22.

- [39] Simell PA, Hirvensalo EK, Smolander VT. Steam reforming of gasification gas tar over dolomite with benzene as a model compound. *Industrial & Engineering Chemistry Research*. 1999;38:1250-7.
- [40] Wang D, Czernik S, Chornet E. Production of Hydrogen from Biomass by Catalytic Steam Reforming of Fast Pyrolysis Oils. *Energy & Fuels*. 1998;12:19-24.
- [41] Baker RTK, Harris PS, Thomas RB, Waite RJ. Formation of filamentous carbon from iron, cobalt and chromium catalyzed decomposition of acetylene. *Journal of Catalysis*. 1973;30:86-95.
- [42] Baker RTK, Alonzo JR, Dumesic JA, Yates DJC. Effect of the surface state of iron on filamentous carbon formation. *Journal of Catalysis*. 1982;77:74-84.
- [43] Tibbetts GG, Devour MG, Rodda EJ. An adsorption-diffusion isotherm and its application to the growth of carbon filaments on iron catalyst particles. *Carbon*. 1987;25:367-75.
- [44] Tibbetts GG. Why are carbon filaments tubular? *Journal of Crystal Growth*. 1984;66:632-8.
- [45] Hata K, Futaba DN, Mizuno K, Namai T, Yumura M, Iijima S. Water-Assisted Highly Efficient Synthesis of Impurity-Free Single-Walled Carbon Nanotubes. *Science*. 2004;306:1362-4.
- [46] Tessonnier J-P, Su DS. Recent Progress on the Growth Mechanism of Carbon Nanotubes: A Review. *ChemSusChem*. 2011;4:824-47.
- [47] Dasgupta K, Joshi JB, Banerjee S. Fluidized bed synthesis of carbon nanotubes – A review. *Chemical Engineering Journal*. 2011;171:841-69.
- [48] Martínez-Hansen V, Latorre N, Royo C, Romeo E, García-Bordejé E, Monzón A. Development of aligned carbon nanotubes layers over stainless steel mesh monoliths. *Catalysis Today*. 2009;147, Supplement:S71-S5.
- [49] DiLeo RA, Landi BJ, Raffaele RP. Purity assessment of multiwalled carbon nanotubes by Raman spectroscopy. *Journal of Applied Physics*. 2007;101:064307-5.
- [50] Saito R, Gruneis A, Samsonidze GG, Brar VW, Dresselhaus G, Dresselhaus MS, et al. Double resonance Raman spectroscopy of single-wall carbon nanotubes. *New Journal of Physics*. 2003;157.1-.15.
- [51] Kastner J, Pichler T, Kuzmany H, Curran S, Blau W, Weldon DN, et al. Resonance Raman and infrared spectroscopy of carbon nanotubes. *Chemical Physics Letters*. 1994;221:53-8.

[52] Herrera JE, Resasco DE. In situ TPO/Raman to characterize single-walled carbon nanotubes. *Chemical Physics Letters*. 2003;376:302-9.

Table 1. Experimental results from toluene reforming

Toluene (g min ⁻¹)	0.01	0.01	0.01	0.01	0.01	0.07
Catalyst (g)	0.0	0.0	0.8	0.0	0.8	0.8
Water (g min ⁻¹)	0.00	0.01	0.01	0.10	0.05	0.02
S/C ratio*	0.0	0.7	0.7	7.3	3.7	0.2
Gas yield (wt.%)	16.1	58.4	105.5	23.2	69.0	36.3
Carbon conversion to CNTs (wt.%)	43.8	<5	56.9	-	-	70.4
Hydrogen production (mmol H ₂ g ⁻¹ toluene)	22.9	24.8	54.8	18.3	30.9	35.6
Gas concentration (vol.%)						
CO	11.0	35.1	31.5	23.9	26.7	18.5
H ₂	85.1	58.4	66.0	72.6	61.8	77.4
CO ₂	2.0	6.0	1.4	1.8	11.4	1.7
CH ₄	1.9	0.6	1.1	1.7	0.1	2.5
C ₂ -C ₄	0.0	0.0	0.0	0.0	0.0	0.0

* S/C means steam to carbon (in toluene) molar ratio

Figure Captions:

Fig. 1. Schematic diagram of the experimental system

Fig. 2. SEM micrographs of stainless steel mesh derived from various reaction conditions: (a) No catalyst + no water; (b) No catalyst + 0.01 g min^{-1} water; (c) and (d) Ni-Mg-Al + 0.01 g min^{-1} water

Fig. 3. SEM micrographs of stainless steel mesh derived from various reaction conditions: (a) Ni-Mg-Al catalyst + 0.05 g min^{-1} water; (b) No catalyst + water 0.1 g min^{-1}

Fig. 4. TEM micrographs of the CNTs produced from toluene gasification in the presence of the Ni-Mg-Al catalyst with water injection rate of 0.01 g min^{-1}

Fig. 5. Raman analysis of the CNTs on the surface of the used stainless steel mesh. (a) No catalyst + no water; (b) No catalyst + 0.01 g min^{-1} water; (c) Ni-Mg-Al + 0.01 g min^{-1} water

Fig. 6. Temperature programmed oxidation results of the CNTs derived from toluene gasification. (a) no catalyst + no water; (b) no catalyst + 0.01 g min^{-1} water; (c) Ni-Mg-Al + 0.01 g min^{-1} water

Fig. 7. EDXS analysis of the CNTs produced with: (a) No catalyst + no water; (b) Ni-Mg-Al + 0.01 g min^{-1} water

Fig. 8. SEM micrographs of CNTs from toluene reforming with higher toluene feeding rate

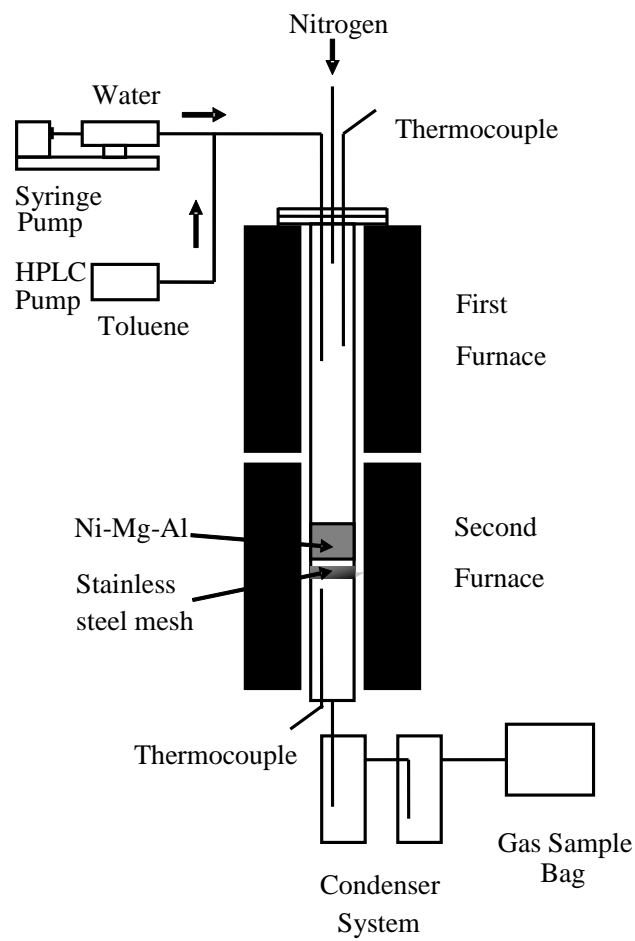


Fig. 1. Schematic diagram of the experimental system

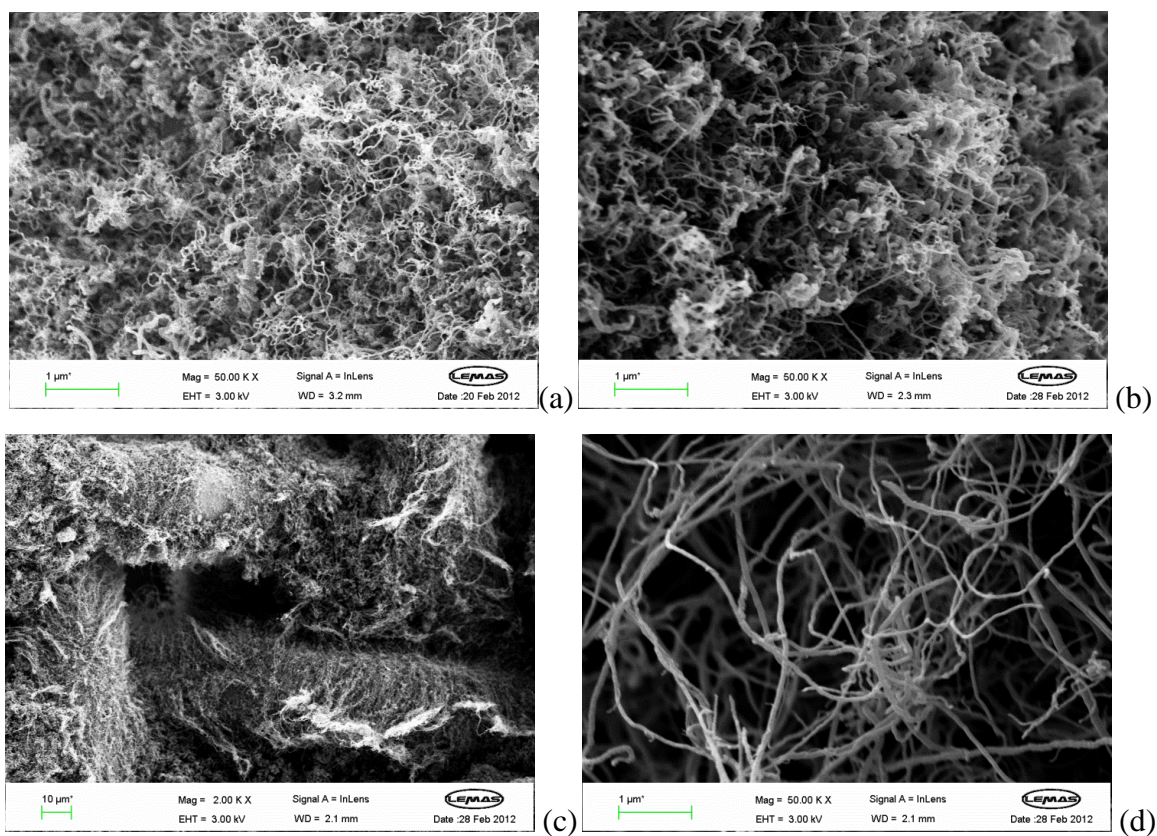


Fig. 2. SEM micrographs of stainless steel mesh derived from various reaction conditions: (a) No catalyst + no water; (b) No catalyst + 0.01 g min^{-1} water; (c) and (d) Ni-Mg-Al + 0.01 g min^{-1} water

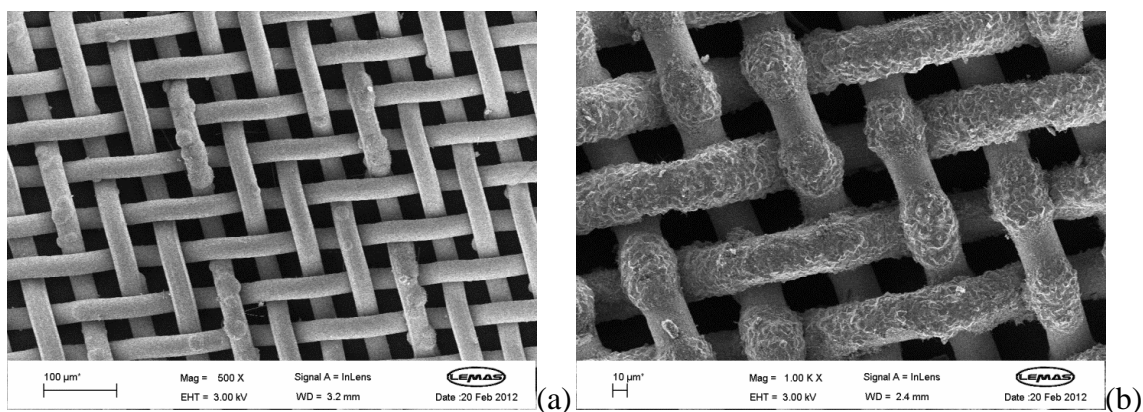


Fig. 3. SEM micrographs of stainless steel mesh derived from various reaction conditions: (a) Ni-Mg-Al catalysyt + 0.05 g min^{-1} water; (b) No catalysyt + water 0.1 g min^{-1}

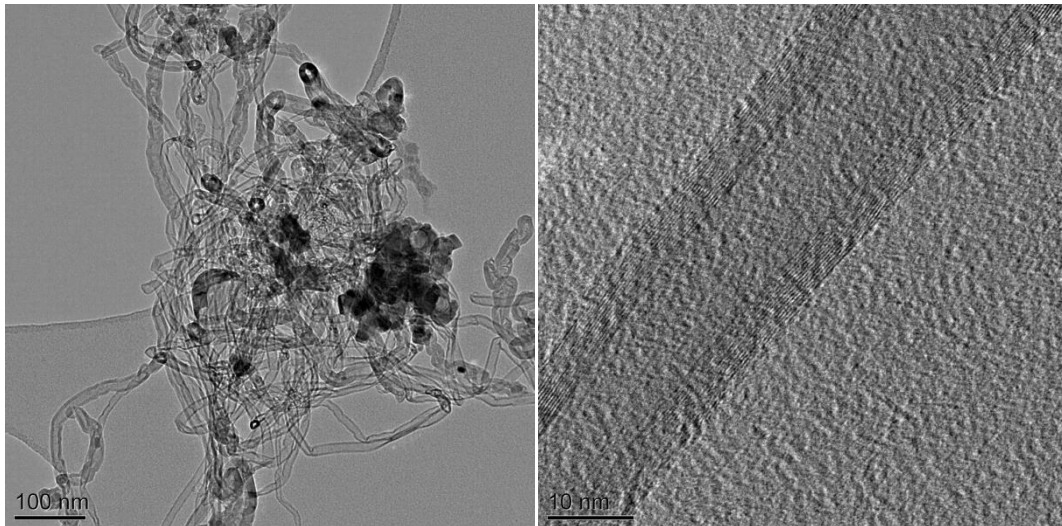


Fig. 4. TEM micrographs of the CNTs produced from toluene gasification in the presence of the Ni-Mg-Al catalyst with water injection rate of 0.01 g min^{-1}

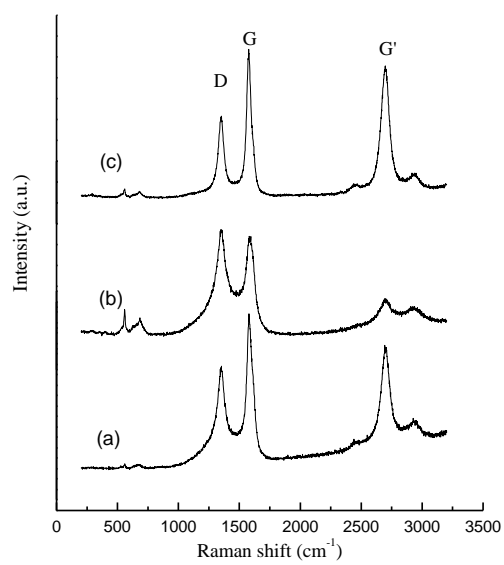


Fig. 5. Raman analysis of the CNTs on the surface of the used stainless steel mesh. (a) No catalyst + no water; (b) No catalyst + 0.01 g min^{-1} water; (c) Ni-Mg-Al + 0.01 g min^{-1} water

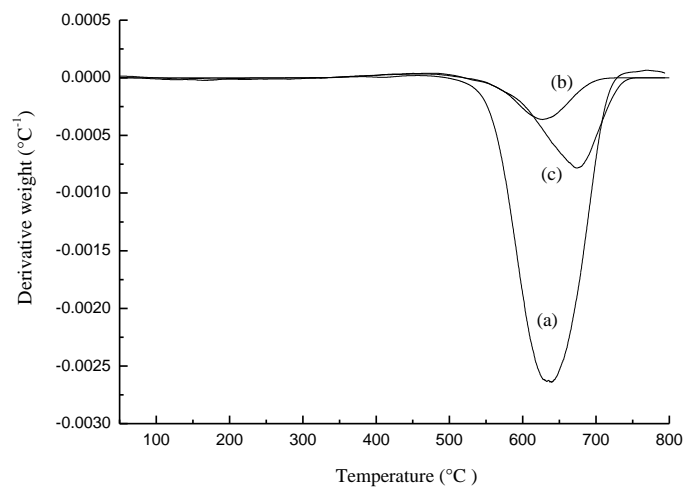


Fig. 6. Temperature programmed oxidation results of the CNTs derived from toluene gasification. (a) no catalyst + no water; (b) no catalyst + 0.01 g min^{-1} water; (c) Ni-Mg-Al + 0.01 g min^{-1} water

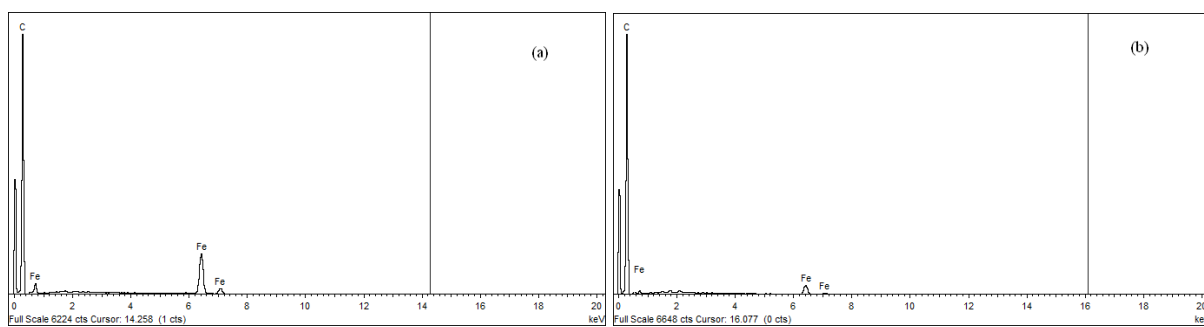


Fig. 7. EDXS analysis of the CNTs produced with: (a) No catalyst + no water; (b) Ni-Mg-Al + 0.01 g min⁻¹ water

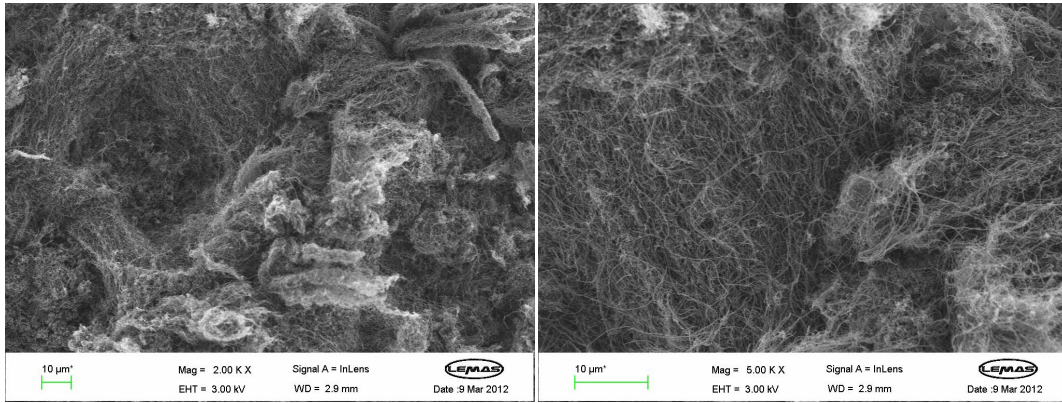


Fig. 8. SEM micrographs of CNTs from toluene reforming with higher toluene feeding rate